Proceedings in MANUFACTURING SYSTEMS

Proceedings in Manufacturing Systems, Volume 8, Issue 4, 2013 ISSN 2067-9238

EMPIRICAL MODEL OF THE CUTTING FORCES IN MILLING

Corina CONSTANTIN[1], George CONSTANTIN[2,*]

1) Eng., PhD, Metallurgical Enterprise for Aeronautics METAV, Bucharest, Romania
2) PhD, Prof, Machine and Production Systems Department, University "Politehnica" of Bucharest, Romania

Abstract: *The paper deals with some aspects of modeling milling force as approach of the integration of multiple modeling in cutting, trying to bring some original aspects in the empirical approach. Within the experimental researches several experiments were conducted on the following types of materials: steel (OLC 45 improved), aluminium alloy (7178), grey cast iron, and titanium (purity 99%). The experimental research in milling with one tooth on 180º were made on a vertical machining centre, FIRST MCV 300, with three axes, in the laboratory of Machine Tools of Machines and Manufacturing Systems Department, Engineering and Management of Technological Systems, University "Politechnica" of Bucharest. The main purpose of the work is to obtain functions of two variables (cutting depth a_p and feed per tooth f_z) for coefficients K_n and K_t (specific forces) by multiple regression. They are integrated in the tangential and normal forces F_t and F_n expressions. The corresponding diagrams of K_n and K_t based on the mathematical model are compared to those determined by experiments for the four materials studied. Some comparison charts for F_x and F_y measured and simulated using the mathematical model established are finally presented, resulting a good approximation. Several conclusions regarding modeling are drawn.*

Key words: *milling, milling cutter, specific cutting force components, tangential cutting force, normal cutting force, cutting force on axis, measured force, simulated force, comparison*.

1. INTRODUCTION

In the milling process, which is one of the processes most widely used in the metal processing industry, even if it has been studied in numerous scientific papers, including papers, interesting and important aspects of the study still remain.

The paper aims to study the field of modelling and simulation of machining process by milling with application to the cutting forces and trying to bring some novelty items by defining new force models used for integrated modelling (CAD model; FEM model; model of cutting forces; dynamic model of cutting; solid bodies machining system model [1]) and simulation that puts together ways and means of distinct domains. This paper responds to a necessity of implementation of items in theoretical and applied a concept to provide a solution for replacing cutting tests expensive and time consuming.

Effective methods for estimating stable processes have been developed in the last decades of Altintas [2], Faassen [3] etc. An essential component of these methods is the development of a model, in fact a differential equation, which has to be adjusted, aiming to reproduce the local characteristics of the cutting system. By combining the mathematical model with a process model can effectively identify the processing parameters.

[*] Corresponding author: Splaiul Independenței 313, Sector 6, 060042, Bucharest, Romania;
Tel.: +40 21 402 9174
E-mail addresses: *corina11@gmail.com* (C. Constantin), *george.constantin@icmas.eu* (G. Constantin)

2. MODEL OF THE CUTTING FORCES − CFM

In order to achieve the cutting force model, one starts from the geometric representation of the tool and workpiece (Fig. 1). It is considered the workpiece moving with the feed speed v_f (case of up milling) and the cutting tool with only one tooth engaged in cutting (tooth j). A point on the cutting edge describes a trajectory (dashed line). On the drawing it is highlighted the previous trajectory (of tooth j − 1), although of the current tooth j. The feed per tooth f_z is sown, being measured between the points of intersection of the trajectories and $j-1$ and j with the axis X.

The angular position of the tooth is variable in time and denoted by ϕ_j (t). Also, the angle described by the tooth a cutting depth a_e and the tool diameter D is denoted by Ω.

The cutting force F_j, which acts on the current tooth, is broken down into two components-the tangential F_{tj} and normal F_{nj}.

The mathematical model of cutting forces in milling describes essentially the material resistance in cutting.

For the determination of mathematical model of the working forces at the milling is necessary to know the surface of contact between tool and workpiece material (A_c). In principle, for an axial element of length dz, it is considered normal to direction Z the chip length l_c. With the two variables, the uncut chip thickness h_c is determined. To highlight the influence of the thickness of the chip in the process of cutting, this is linked with the cutting depth a_p and the feed per tooth f_z and current angle of the tooth φ(t).

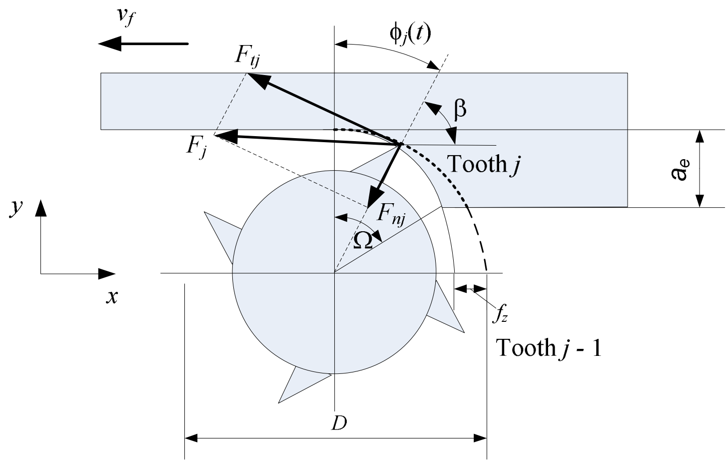

Fig. 1. Representation of cutting forces in milling (up milling).

Table 1

Values of the cutting force components and specific forces after (13)

Nr.	Angular in-crement [rad]	Angle φ [rad]	Time [s]	F_x	F_y	F_z	K_t	K_n
0	0.0628	0	69.429	3.61633	42.6636	53.7872	-904083	10665900
1	0.0628	0.0628	69.43	4.71497	61.2946	125.839	-3401.47	24212.25
2	0.0628	0.1256	69.431	-73.288	107.437	124.603	11815.51	23086.1
3	0.0628	0.1884	69.432	-31.1737	31.6315	109.039	3295.063	4924.366
4	0.0628	0.2512	69.433	-27.3743	26.0925	93.7042	2013.71	3225.035
5	0.0628	0.314	69.434	-21.3776	34.5612	90.5457	781.4584	3194.109
6	0.0628	0.3768	69.435	-28.0151	37.262	81.7566	838.178	3053.747
7	0.0628	0.4396	69.436	-61.0199	34.1034	86.0138	2390.631	3337.672
8	0.0628	0.5024	69.437	-77.2705	34.2407	79.9713	2659.483	3489.158
9	0.0628	0.5652	69.438	-80.9784	36.3922	88.3484	2281.896	3458.447
10	0.0628	0.628	69.439	-72.5098	29.8462	95.4895	1750.305	2840.036
11	0.0628	0.6908	69.44	-80.658	17.1204	95.6268	2010.956	2533.888
12	0.0628	0.7536	69.441	-89.6301	8.14819	98.1445	2184.05	2457.58
13	0.0628	0.8164	69.442	-86.38	5.67627	99.3347	1887.505	2292.654
14	0.0628	0.8792	69.443	-82.4432	-9.16E-02	103.638	1708.77	2059.014
15	0.0628	0.942	69.444	-89.0808	-8.88062	109.909	1841.533	2065.404
16	0.0628	1.0048	69.445	-92.926	-15.4724	116.18	1862.669	2077.264
17	0.0628	1.0676	69.446	-83.7708	-16.1591	113.113	1556.704	1871.794
18	0.0628	1.1304	69.447	-84.1827	-25.4974	113.113	1629.167	1804.082
19	0.0628	1.1932	69.448	-83.9539	-32.7301	118.24	1650.649	1774.235
20	0.0628	1.256	69.449	-77.3163	-42.5262	111.923	1692.501	1586.667
21	0.0628	1.3188	69.45	-72.8302	-51.6357	117.279	1759.636	1488.351
22	0.0628	1.3816	69.451	-74.5697	-52.597	112.93	1671.87	1612.421
23	0.0628	1.4444	69.452	-67.8864	-58.6395	120.85	1681.631	1510.852
24	0.0628	1.5072	69.453	-58.7311	-68.7561	119.293	1812.394	1358.805
25	0.0628	1.57	69.454	-47.9736	-66.6504	123.596	1667.215	1198.013
26	0.0628	1.6328	69.455	-42.8009	-74.8444	122.91	1804.691	1186.194
27	0.0628	1.6956	69.456	-33.4625	-76.9958	124.008	1819.966	1078.065
28	0.0628	1.7584	69.457	-25.8636	-84.8694	121.49	1999.027	1049.392
29	0.0628	1.8212	69.458	-19.9585	-80.1086	120.621	1875.142	1011.227
30	0.0628	1.884	69.459	-15.4724	-83.9539	118.561	1973.638	1066.585
31	0.0628	1.9468	69.46	-8.92639	-74.5239	119.98	1775.067	958.7228
32	0.0628	2.0096	69.461	0	-81.2988	123.184	2032.565	953.9233
33	0.0628	2.0724	69.462	5.8136	-75.7141	118.423	1972.663	892.7239
34	0.0628	2.1352	69.463	15.5182	-71.5942	118.79	2035.599	745.2515
35	0.0628	2.198	69.464	24.7192	-67.5201	125.061	2136.094	605.5966
36	0.0628	2.2608	69.465	34.1034	-59.8755	118.698	2200.744	382.8911
37	0.0628	2.3236	69.466	41.153	-63.1256	115.768	2542.23	449.693
38	0.0628	2.3864	69.467	43.7164	-54.7028	110.962	2528.85	359.9145
39	0.0628	2.4492	69.468	48.8892	-50.8118	110.458	2744.317	309.4522
40	0.0628	2.512	69.469	48.2483	-46.0052	105.698	2806.277	372.6277
41	0.0628	2.5748	69.47	53.2837	-35.1105	105.103	2971.224	47.0628
42	0.0628	2.6376	69.471	59.3719	-32.7759	100.571	3511.426	1.469453
43	0.0628	2.7004	69.472	51.5442	-23.1628	102.631	3308.488	-62.3942
44	0.0628	2.7632	69.473	51.6815	-20.0958	91.095	3753.338	-28.3173
45	0.0628	2.826	69.474	51.8188	-3.84521	88.1653	4065.062	-1001.35
46	0.0628	2.8888	69.475	53.1464	2.38037	87.8906	5085.949	-1559.64
47	0.0628	2.9516	69.476	49.9878	3.20435	83.1757	6421.491	-1667.12
48	0.0628	3.0144	69.477	43.7164	11.3525	89.2639	8268.823	-3314.82
49	0.0628	3.0772	69.478	59.2346	2.92969	152.939	22927.94	-2620.79
50	0.0628	3.14	69.479	155.09	-41.6107	110.092	2598663	692787.3

Table 2

Values of specific forces components determined after (13) for all records of tests for steel OLC45 improved

a_p	f_z	v_c	K_t	K_n	ζ
0.5	0.08	150	2310.929402	1385.90152	0.5997161
0.5	0.092	165	3112.501012	1517.55514	0.4875678
0.5	0.105	181.5	2555.945195	1453.60014	0.5687133
0.5	0.121	199.6	2737.997835	1314.45797	0.48008
0.63	0.08	150	3065.518054	1765.95413	0.5760704
0.63	0.092	165	3197.288272	1611.88477	0.5041412
0.63	0.105	181.5	3303.024635	1744.21797	0.5280669
0.63	0.121	199.6	2557.25863	674.469114	0.2637469
0.78	0.08	150	2842.022369	1839.28586	0.647175
0.78	0.092	165	3281.699603	1796.91343	0.5475557
0.78	0.105	181.5	3066.94361	1747.68763	0.5698467
0.78	0.121	199.6	2997.573491	1789.55263	0.5970004
0.97	0.08	150	3050.03338	2007.36936	0.6581467
0.97	0.092	165	3240.32	1994.2581	0.615451
0.97	0.105	181.5	3400.195272	2136.43315	0.6283266
0.97	0.121	199.6	3321.2341	2021.4532	0.6086452

$$h_c(t) = h_{cm}(ap, f_z)\cdot\sin\varphi(t)\,, \tag{1}$$

where $h_{cm}(a_p, f_z)$ represents a relation previously determined [4, 5].

The component F_x of the cutting force will be considered as a function of the tangential and normal components projections, the current angle of the tooth becoming

$$F_x(t) = f(F_t, F_n, \varphi(t))\,. \tag{2}$$

The components F_t and F_n shall be regarded as functions of the chip area A_c and empirically determined coefficients for the two tangential directions K_t and normal K_n, respectively, whose functions are given by the relations

$$\begin{aligned} F_t(t) &= K_t A_c(t); \\ F_n(t) &= K_n A_c(t). \end{aligned} \tag{3}$$

where the surface of undeformed chip is considered as a function of time by

$$A_c(t) = l_c\, h_c(t). \tag{4}$$

The model proposed is different from that found in the literature (see [6 and 7]) in which the instantaneous chip thickness is approximated using the static part, namely the feed per tooth f_z, in that it can take into account the average chip thickness h_{cm} [1, 2]. Also, the model might not use the cutting depth a_p, but the chip surface length l_c determined by relation [4, 5].

$$h_c(t) = f_z\cdot\sin\varphi(t)\,, \tag{5}$$

But, if we relate strictly to the relation (3), one can restrict the chip surface relationship A_c variable in time at that given by [4, 5]

$$A_c = (a_1 + a_2\, a_p + a_3\, f_z)\sin\varphi(t). \tag{6}$$

The next stage is that of determining the coefficients that appear in the tangential and normal components expressions (or radial) of the cutting force on tooth.

It can be seen that the values of the coefficient K_t can be obtained from the expression of force F_t if it becomes maximum. For tangential direction, the force F_t becomes maximum for an angle $\varphi = \pi/2$, when it is equal to the

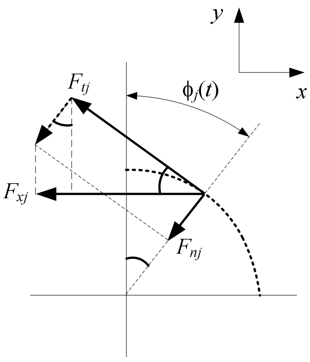

Fig. 2. The scheme of the forces for determining component F_x of the cutting force in milling.

maximum value of the cutting force in the direction of Y, namely $F_{y\max}$.

The tangential and normal forces expressions are given by

$$\begin{aligned} F_t &= K_t a_p f_z\cdot\sin\varphi(t); \\ F_n &= K_n a_p f_z\cdot\sin\varphi(t). \end{aligned} \tag{7}$$

According to Fig. 2, components on axes X and Y of the cutting force are coming from the two components of the cutting force on the tooth, tangential force F_t and the normal F_n, projected onto the two directions and added together, resulting the relations (8).

$$\begin{aligned} F_x &= -F_t\cos\varphi(t) - F_n\sin\varphi(t) = -a_p f_z\cdot\sin\varphi(t)[-K_t\cdot\cos\varphi(t) - K_n\cdot\sin\varphi(t)]; \\ F_y &= -F_t\sin\varphi(t) + F_n\cos\varphi(t) = a_p f_z\cdot\sin\varphi(t)[-K_t\cdot\sin\phi(t) + K_n\cdot\cos\varphi(t)]. \end{aligned} \tag{8}$$

Relations (7) are valid for $\varphi(t) \in [0, \pi]$. For generalization, it introduces a function of state $s(t)$ which enables the expressions on the interval $[0, \pi]$ and disables, settling them at the value 0 outside it

$$s(t) = \begin{cases} 1, & \varphi(t)\in[0,\pi] \\ 0, & \varphi(t)\in(\pi, 2\pi] \end{cases}. \tag{9}$$

In the end, we get

$$\begin{aligned} F_x &= s(t)\{-F_t\cos\varphi(t) - F_n\sin\varphi(t) = -a_p f_z\cdot\sin\varphi(t)[-K_t\cdot\cos\varphi(t) - K_n\cdot\sin\varphi(t)]\}; \\ F_y &= s(t)\{-F_t\sin\varphi(t) + F_n\cos\varphi(t) = a_p f_z\cdot\sin\varphi(t)[-K_t\cdot\sin\phi(t) + K_n\cdot\cos\varphi(t)]\}. \end{aligned} \tag{10}$$

In processing with the depth $a_e = D$, as is the case, the two specific forces K_n and K_t can be considered as being in a constant ratio

$$\frac{F_r}{F_t} = \zeta, \tag{11}$$

To determine the specific forces, one starts from the experimental determinations of components of the cutting force on X, Y, and Z, i.e. F_x, F_y, F_z under the conditions specified for a_p, f_z and v_c (n, respectively). If it is considered a point in cutting characterised by angular position φ_i (where $0 \le \varphi_i \le \pi$), then we can get expressions of tangential and normal (radial) components of the cutting force based on the scheme of Fig. 2 as follows:

$$\begin{aligned} F_t &= -F_x \cos\varphi_i - F_y \sin\varphi_i; \\ F_n &= -F_x \sin\varphi_i + F_y \cos\varphi_i. \end{aligned}, \tag{12}$$

On the basis of the tangential and normal components given by expressions (7) and (12), one determines the tangential and normal specific force expressions of forms

$$\begin{aligned} K_t &= \frac{F_t}{A_c(\varphi)} = \frac{F_t}{a_p f_z \cdot \sin\varphi(t)}; \\ K_n &= \frac{F_n}{A_c(\varphi)} = \frac{F_n}{a_p f_z \cdot \sin\varphi(t)}. \end{aligned} \tag{13}$$

Table 1 presents the experimental determinations (52 records) for cutting force components F_x, F_y, F_z in the specific conditions a_p = 0.5 mm, f_z = 0.08 mm/tooth and v_c = 150 m/min, accompanied by the specific forces values determined in accordance with the relationship (7). The points to the extremities were removed from the set, where excess values occur with much variation in normal, produced by vibration, the system dynamics respectively. The following average values are given by

$$\begin{aligned} K_t &= 2310.929\,[\text{N/mm}^2] \\ K_n &= 1385.902\,[\text{N/mm}^2]. \end{aligned} \tag{14}$$

To be able to be used in the dynamic model of the cutting force in the milling, these values must be validated. The measured values of cutting force components are compared with those forces simulated (calculated) on the basis of the relation (7) in which the parameters a_p = 0.5 mm, f_z = 0.08 mm/tooth, v_c = 150 m/min and K_t = 2639.918 N/mm^2 were introduced. The variation of component F_x depending on the angle φ_i described by a point on the cutting edge is presented in Fig. 3. Comparison charts are shown in Figs. 4 and 5 for F_x and F_y rspectively.

There is a good approximation of the measured values by modelling. Some larger differences are found to angles with higher values $3\pi/4$, and evidently at tooth entry and exit to and from cutting, which produces dynamic phenomena.

Table 2 presents the values of specific forces obtained after (13) for all records of the experimental plan for the workpiece of OLC45 improved. For these values two functions have been determined by multiple regression, $K_n = f\,({}_p a, f_{,x}, v_{,c})$ and $K_t = f\,({}_p a, f_{,x}, v_{,c})$ of form

$$\begin{aligned} K_t &= -41.224 \cdot a_p^{0.2769} \cdot f_{z_z}^{-17.773} \cdot v_c^{26.149}\ [\text{N/mm}^2]; \\ K_n &= -876.594 \cdot a_p^{0.6203} \cdot f_{z_z}^{-218.988} \cdot v_c^{307.873}\ [\text{N/mm}^2]. \end{aligned} \tag{15}$$

The diagrams corresponding to relation (13) are shown in Figs. 6 and 7.

From the study of specific force in milling one ascertains that it depends on the uncut chip thickness (or in terms of process parameters on cutting depth a_p and ad feed per tooth f_z) and also on speed v_c. It increases with

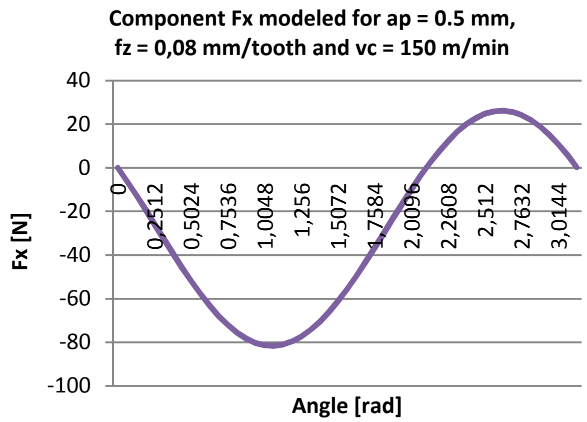

Fig. 3. Change in component F_x (force modeled, OLC 45).

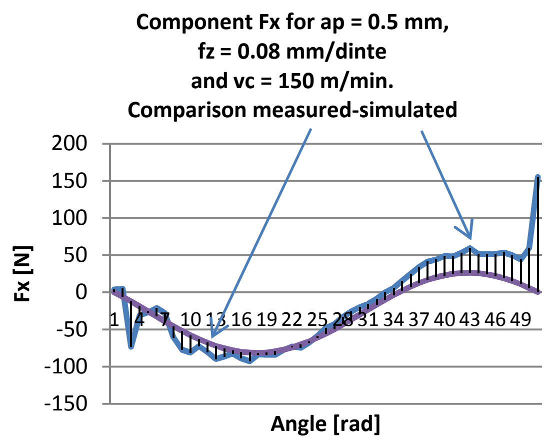

Fig. 4. Comparison diagrams of component F_x (measuerd-simulated).

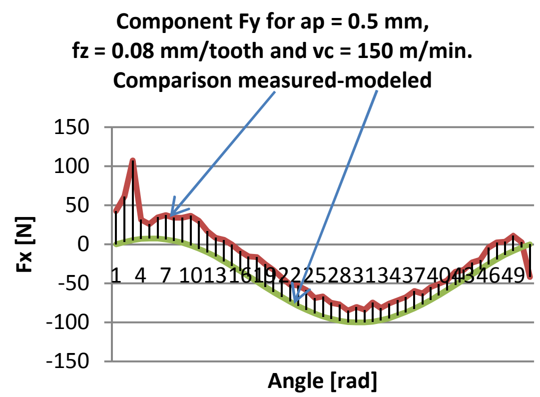

Fig. 5. Comparison diagrams of component F_y (measuerd-simulated).

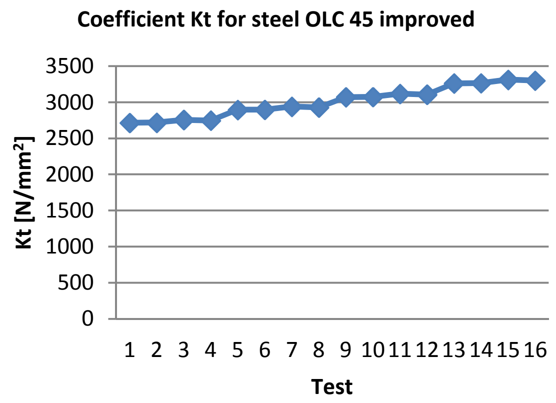

Fig. 6. Variation diagram of coefficient K_t (after (13)).

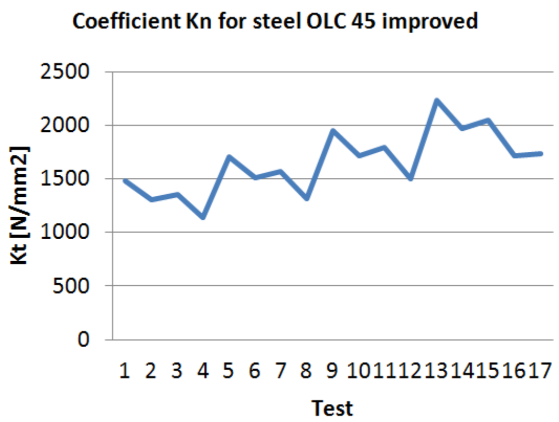

Fig. 7. Variation diagram of coefficient K_n (after (13)).

the thickness of the chip reduction and decreases slightly with increasing cutting speed.

For these values representing the values of specific force components determined by (13) for all records in the tests or OLC45 improved steel, two functions have been determined by multiple regression, $K_n = f(a_p, f_x, v_c)$ and $K_t = f(a_p, f_x, v_c)$, in the form of relationships (16).

$$K_t = -5.5768 \cdot a_p^{-0.5762} \cdot f_{z_z}^{-2.3147} \cdot v_c^{2.9247} \text{ [N/mm}^2\text{]};$$
$$K_n = -125.4540 \cdot a_p^{0.1754} \cdot f_{z_z}^{-30.7831} \cdot v_c^{43.5811} \text{ [N/mm}^2\text{]}. \qquad (16)$$

The corresponding relationship diagrams (13) for titanium compared to those determined on the basis of the functions (16) shown in Figs. 8 and 9.

For the values of the specific force components determined by (13) for all records for tests on cast iron, two functions have been determined by multiple regression, $K_n = f(a_p, f_x, v_c)$ and $K_t = f(a_p, f_x, v_c)$ in the form of relations (17).

$$K_t = 92193.44 \cdot a_p^{-0.5831} \cdot f_{z_z}^{-0.3257} \cdot v_c^{-0.8129} \text{ [N/mm}^2\text{]};$$
$$K_n = 867560.96 \cdot a_p^{0.2234} \cdot f_{z_z}^{-0.7645} \cdot v_c^{-1.4534} \text{ [N/mm}^2\text{]}. \qquad (17)$$

The diagrams corresponding to relationship (13) for cast iron compared to those determined on the basis of the functions (17) are shown in Figs. 10 and 11.

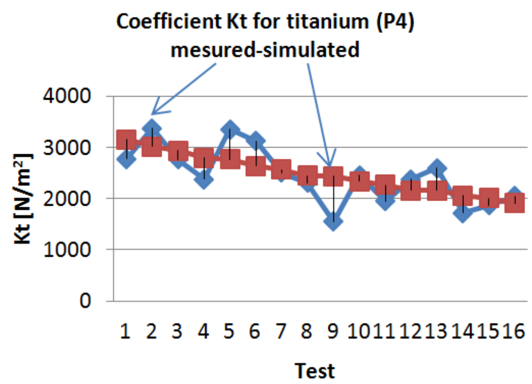

Fig. 8. Variation diagram of coefficient K_t (given by (13)) and simulated for titanium.

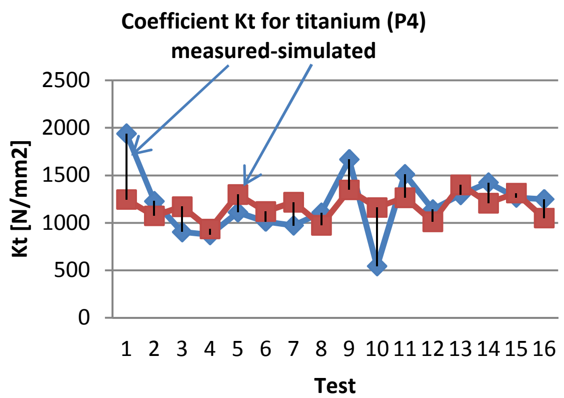

Fig. 9. Variation diagram of coefficient K_n (given by (13)) and modeled for titanium.

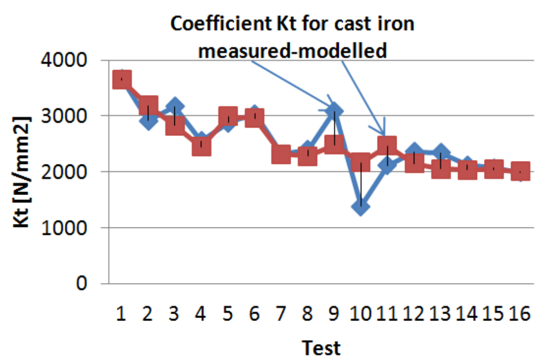

Fig. 10. Variation diagram of coefficient K_t (given by (13)) and modeled for cast iron.

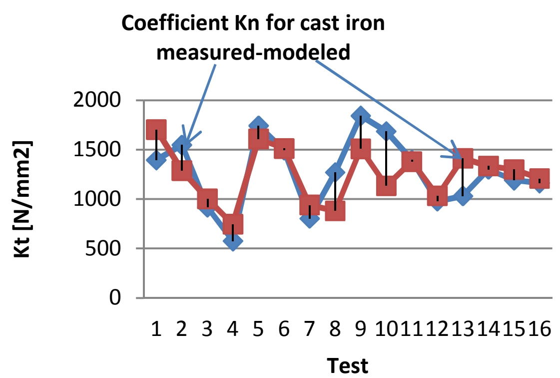

Fig. 11. Variation diagram of coefficient K_n (given by (13)) and modeled for cast iron.

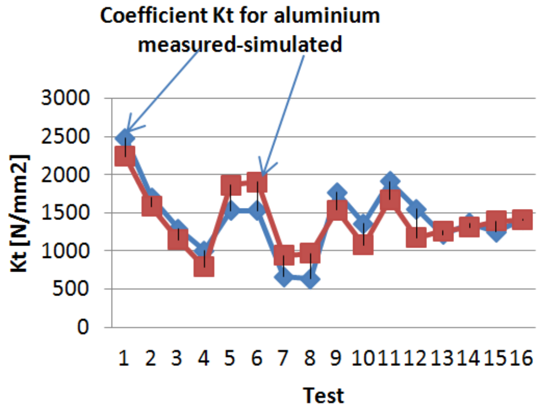

Fig. 12. Variation diagram of coefficient K_t (given by (13)) and modeled for Al 7178.

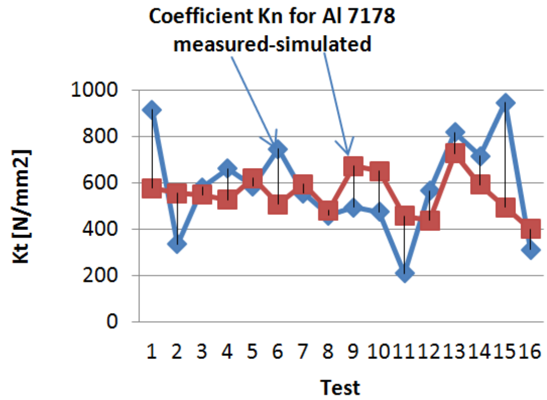

Fig. 13. Variation diagram of coefficient K_n (given by (13)) and modeled for Al 7178.

For the values of specific force components determined by (13) for all records of tests for aluminium two functions have been determined by multiple regression, $K_n = f(a_p, f_x, v_c)$ and $K_t = f(a_p, f_x, v_c)$ in the form of relations (18)

$$K_t = 288004981.74 \cdot a_p^{0.0019} \cdot f_{z_z}^{-0.7263} \cdot v_c^{-2.4906}\ [\text{N/mm}^2];$$
$$K_n = 0.4378244 \cdot a_p^{-0.0299} \cdot f_{z_z}^{-0.5327} \cdot v_c^{1.1006}\ [\text{N/mm}^2]. \quad (18)$$

The comparison diagrams corresponding to relation (13) for aluminium when compared to those determined on the basis of the functions (18) are shown in Figs. 12 and 13.

Some comparison charts for F_x and F_y measured and modeled for iron, titanium and Al 718 are presented in Figs. 14–19. There is a good approximation of the measured values by modelling. Some differences are the larger at angles with values greater than $3\pi/4$, and evidently at tooth entry and exit to and from cutting, which produces dynamic phenomena.

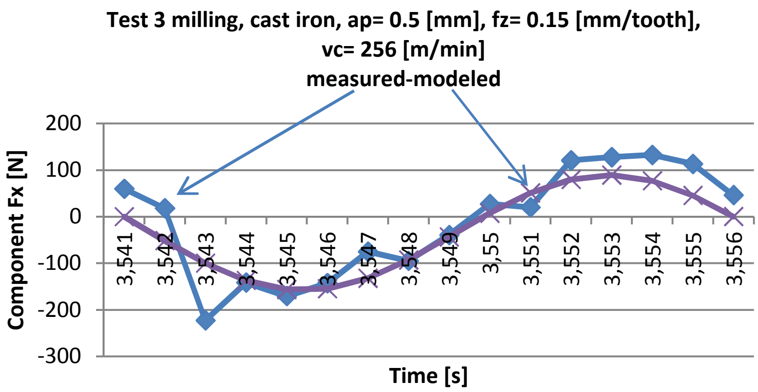

Fig. 14. Comparison diagrams of component F_x (measured-modeled) for cast iron.

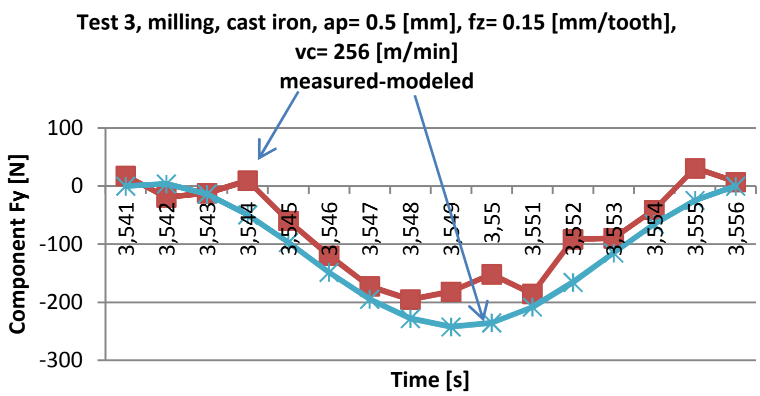

Fig. 15. Comparison diagrams of component F_y (measured-modeled) for cast iron.

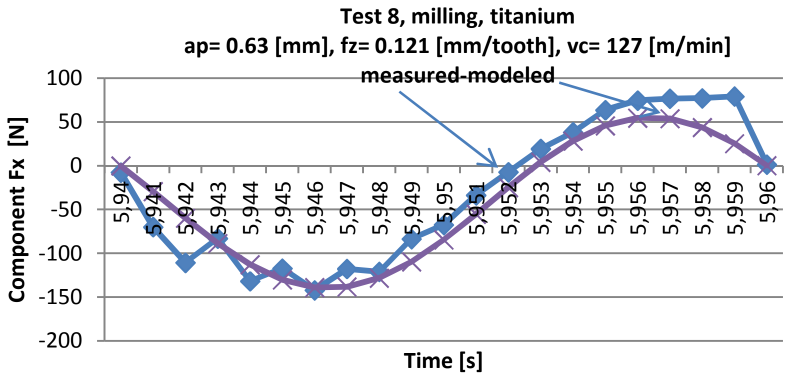

Fig. 16. Comparison diagrams of component F_x (measured-modeled) for titanium.

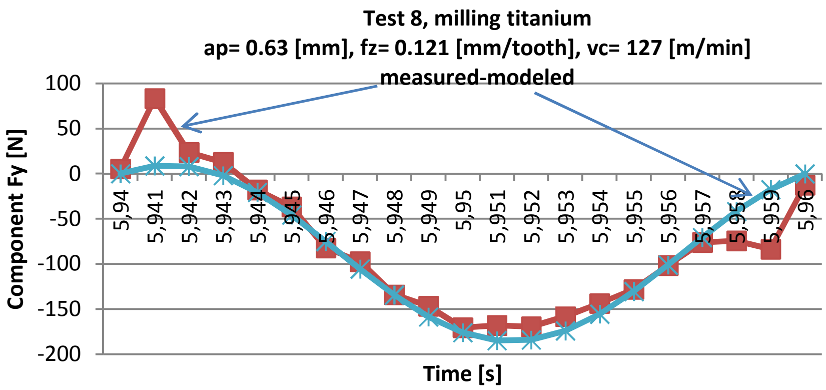

Fig. 17. Comparison diagrams of component F_y (measured-modeled) for titanium.

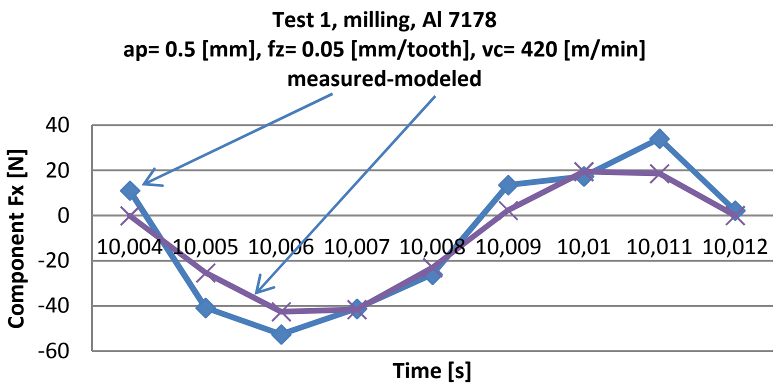

Fig. 18. Comparison diagrams of component F_x (measured-modeled) for cast iron Al 7178.

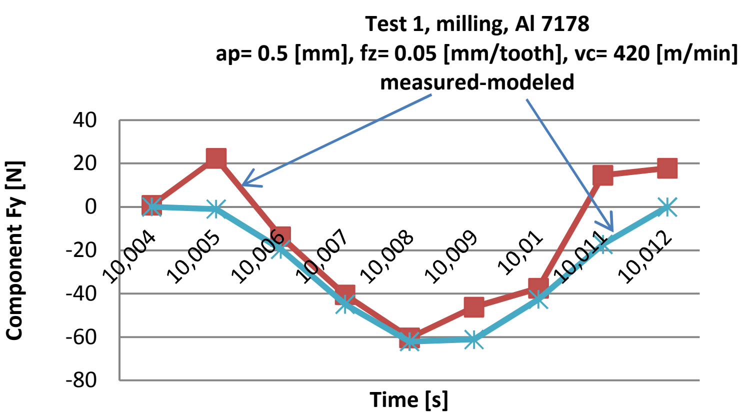

Fig. 19. Comparison diagrams of component F_y measured-modeled) for Al 7178.

3. CONCLUSIONS

The research presented in this paper fall into the theoretical and applied studies of modelling-simulation of cutting process through milling, for the integration and connection of the three types of models of cutting forces in milling with customizing them to four types of the studied materials (steel, cast iron, titanium and aluminium), namely chip geometry model; empirical mathematical model of cutting forces, structural response of processing system with several degrees of freedom).

The integrated modeling method of milling process that has been proposed has been applied for a machine-tool and more processed materials using tools with working regimes chosen in accordance with the manufacturer's indications. The results obtained proved viable for each step of modeling and fits into the area of acceptable or even small errors.

Based on the classic model of the chip geometry presented in [5], method and functions laid down the basis for determination of the cutting force components on the X and Y directions depending on specific K_t and K_n forces and area of uncut chip.

Having as landmark the specific forces components values determined using known relations for all records of the experimental plan and all four types of the studied materials, two functions of exponential form were determined by multiple regression, $K_n = f\ (a_p, f_x, v_c)$ and $K_t = f\ (a_p, f_x, v_c)$. Some values for concrete cutting of the plan of measurements have been entered into force mathematical model and variation of the force curves were compared with measured curves, resulting in a good approximation modeled-measured.

REFERENCES

[1] W.J. Endres, *A Dynamic Model of the Cutting Force System in the Turning Process*, University of Illinois at Urbana-Champaign, 1990.

[2] *Y. Altintaş, M. Weck*, Chatter Stability of Metal Cutting and Grinding, in Annals of the CIRP, vol. 53, no. 2, 2004, pp. 619−642.

[3] R.P. H. Faassen, N. van de Wouw, J.A.J. Oosterling, H. Nijmeijer, *Prediction of regenerative chatter by modelling and analysis of high–speed milling, in International Journal of Machine Tools and Manufacture*, vol. 43, 2003, pp. 1437−1446.

[4] C. Constantin, *Cercetări privind modelarea şi simularea procesului de aşchiere* (Researches regarding modelling and simulation of the cutting process applied to milling), PhD Thesis, University „Politehnica” of Bucharest, 2012.

[5] C. Constantin, G. Constantin, *Aspects regarding modelling the chip geometry in end milling*, Proceedings in Manufacturing Systems, Vol. 7, Is2. 1, 2012, pp. 11−18.

[6] E. Budak, *Analytical models for high performance milling. Part II: Process dynamics and stability*, *International Journal of Machine Tools and Manufacture*, vol. 46, 2006, pp. 1489–1499.

[7] E. Butcher, P. Nindujarla, E. Bueler, S*tability of up- and down-milling using Chebyshev collocation method*, Proceedings of IDETC/CIE 2005, ASME 2005 International Design Engineering Technical Conferences & Computers and Information in Engineering Conference, September 24−28, 2005, Long Beach, California, USA.